Flutter of Turbofan Rotors with Mistuned Blades

Krishna Rao V. Kaza* and Robert E. Kielb†
NASA Lewis Research Center, Cleveland, Ohio

A set of aeroelastic equations describing the motion of an arbitrarily mistuned rotor with flexible, pretwisted, nonuniform blades is developed using an extended Hamilton's principle. The derivation of the equations has its basis in the geometric nonlinear theory of elasticity in which the elongations and shears are negligible compared to unity. A general expression for foreshortening of a blade is derived and is explicitly used in the formulation. The blade aerodynamic loading in the subsonic and supersonic flow regimes is obtained from two-dimensional, unsteady, cascade theories. The aerodynamic, inertial, and structural coupling between the bending (in two planes) and torsional motions of the blade is included. The equations are used to investigate the aeroelastic stability and to quantify the effect of frequency mistuning on flutter in turbofans. Results indicate that a moderate amount of intentional mistuning has enough potential to alleviate flutter problems in unshrouded, high-aspect-ratio turbofans.

Nomenclature

A = cross-sectional area of the blade
A_0 = reference value of A
$[A]$ = aerodynamic matrix
A_j = torsional mode shape
a = elastic axis location
a_0 = speed of sound
B_1, B_2 = blade sectional constants
b, b_R = semichord and reference semichord, respectively
c = blade chord
E = Young's modulus of elasticity
$[E], [\bar{E}_{s,r}]$ = matrices
e = mass and elastic axis offset (also base for natural logarithm)
e_A = area centroid and elastic axis offset
$\bar{e}_x, \bar{e}_y, \bar{e}_z$, $\bar{e}_{x_3}, \bar{e}_{y_3}, \bar{e}_{z_3}$ = unit vectors along x,y,z, and x_3,y_3,z_3 axes, respectively
G = shear modulus of elasticity
$\bar{g}_{si}, \bar{h}_{si}$ = nondimensional amplitudes of generalized coordinates associated with the bending modes W_i of the sth blade measured out of and in the plane of rotation
$\bar{g}_{ari}$ = $\bar{h}_{si} e^{-i\beta_r s}$
$\bar{h}_{ari}$ = $\bar{g}_{si} e^{-i\beta_r s}$
I_{xx}, I_{zz} = bending moment of inertia about the major (parallel to the x axis) and minor axes through centroid
I_{xx0} = reference bending moment of inertia
i = $\sqrt{-1}$
J = torsional stiffness constant
J_0 = reference value for J
k = reduced frequency, $\omega_0 b / V_{\text{eff}} = \omega_0 b / M_{\text{eff}} a_0$
k_m = polar mass radius of gyration about elastic axis, $(k_m^2 = k_{m_1}^2 + k_{m_2}^2)$
k_{m_0} = reference polar radius of gyration of cross-sectional mass about elastic axis
k_{m_1}, k_{m_2} = mass radii of gyration about x and z axes
k_A = polar radii of gyration of cross-sectional area about elastic axis
L = blade length
L_a = lift per unit span, positive up (negative z direction)
$l_{hhr}, l_{h\alpha r}$ = nondimensional lift coefficients due to bending and torsional motions in the rth cascade mode
$l_{\alpha hr}, l_{\alpha\alpha r}$ = nondimensional moment coefficients due to bending and torsional motion in the rth cascade mode
M_{ax} = axial Mach number, $= V_a / a_0$
M_a = aerodynamic moment per unit span about the elastic axis, positive nose up
M_r = relative Mach number, $= \sqrt{V_a^2 + \Omega^2 r^2} / a_0$
M_{eff} = effective relative Mach number, $= V_{\text{eff}} / a_0$
M_g, M_h, M_α = number of generalized coordinates with the bending motions out of and in the plane of rotation and with the torsional motion
$[M]$ = inertial matrix
m = mass per unit length
m_0 = reference mass per unit length
N = number of blades in cascade
P, P' = arbitrary point on the elastic axis before and after deformation
$[P]$ = stiffness matrix, Eq. (16)
p_j = quantity defined in Eq. (4)
$[Q]$ = matrix, Eq. (16)
R_H = hub radius
R_T = blade tip radius
r = integer $(0,1,2,\ldots,N-1)$ specifying mode of a tuned cascade; also, blade coordinate along elastic axis before deformation
r_{α_0} = reference radius of gyration
$\bar{r}_1$ = position vector of an arbitrary point on the blade after deformation
$[S]$ = stiffness matrix
s = integer specifying blade, $= 0,1,2,\ldots,N-1$; also, blade spacing
T_k = kinetic energy
$T_c, \bar{T}_c$ = blade tension, $\bar{T}_c = T_c / m_0 \Omega^2 L^2$
$[T]$ = transformation matrix
t, t_0, t_1 = time, initial time, and final time, respectively
U = strain energy
U_F = radial foreshortening
u, v, w = deformations of elastic axis in X_Ω, Y_Ω, and Z_Ω directions, respectively
V_a = axial velocity
V_{eff} = effective relative velocity, $= \sqrt{V_a^2 + \Omega^2 r^2 \cos[90 - \xi - \tan^{-1}(V_a / \Omega r)]}$

Presented as Paper 82-0726 at the AIAA/ASME/ASCE/AHS 23rd Structures, Structural Dynamics and Materials Conference, New Orleans, La., May 10-12, 1982; submitted May 12, 1982; revision received Aug. 23, 1983. This paper is declared a work of the U.S. Government and therefore is in the public domain.

*Research Scientist. Associate Fellow AIAA.
†Research Engineer. Member AIAA.

W = work done by aerodynamic loading
W_i = beam functions ($i=1,2,...$)
$[\bar{W}], [W]$ = model function matrices
$X_\Omega, Y_\Omega, Z_\Omega$ = hub-fixed axis system, rotates about the Z_Ω axis with an angular velocity Ω
xyz = blade-fixed axis system at arbitrary point on elastic axis
$x_3y_3z_3$ = blade-fixed axis system in the deformed configuration obtained by rotating xyz
$\{X\}, \{Y\}$ = column matrices
$[1]$ = unity matrix
α = angle of twisting deformation, positive when leading edge is upward
α_{si} = amplitudes of generalized coordinates associated with torsional modes A_i of the sth blade ($i=1,2,...$)
α_{ari} = $\alpha_{si}e^{-i\beta_r s}$
β_r = interblade phase angle in the rth mode of tuned cascade, $=2\pi r/N$
γ = nondimensional eigenvalue, $=(\omega/\omega_0)^2$
$\gamma_{yy}, \gamma_{yx}, \gamma_{yz}$ = engineering strain components
$\delta(\ )$ = variation of $(\ )$
$\zeta_{hs1}, ..., \zeta_{\alpha s1}$ = damping ratios of sth blade
$\eta, \bar{\eta}, \eta_a$ = blade running coordinate measured from hub; $\bar{\eta}=\eta/L$; blade elastic axis position; $\eta_a=(a+1)/2$
μ_0 = reference mass ratio, $=m_0/\pi\rho_a b_R^2$
$\bar{\mu}$ = real part of eigenvalue
ξ = pretwist angle
ρ_a, ρ_m = fluid and blade material density
τ = nondimensional time, $t\omega_0$
$\bar{\nu}$ = imaginary part of eigenvalue
Ω = rotational speed
ω, ω_0 = frequency and reference frequency, respectively
ω = angular velocity vector expressed in xyz system

Superscripts

$(\ )$ = derivative $\partial(\ )/\partial t$ or $\partial(\ )/\partial\tau$
$(\ )$ = derivative $\partial(\ )/\partial r$ or $\partial(\ )/\partial\eta$

Introduction

A RESEARCH program in propulsion system aeroelasticity is being conducted at the NASA Lewis Research Center. As a part of this general program, an effort was made by the authors (see Refs. 1 and 2) to improve the physical understanding of turbofan engine aeroelastic characteristics, including blade mistuning (nonidentical blade properties) effects. Other published works on mistuning are cited in Refs. 1 and 2.

The mathematical formulation considered in Ref. 1 is a "typical section" model with two degrees of freedom, bending and pitching about the elastic axis. This model was found to be sufficient to elicit physical understanding of mistuning effects and to conduct parametric studies. Furthermore, this model was utilized in Ref. 3 to show that mistuning has enough potential to raise the flutter speed of an advanced fan significantly. This potential may have a very practical significance in eliminating the commonly used midspan shrouds in advanced turbofan designs. The main purpose of the midspan shrouds is to increase the blade natural frequencies and thus avoid aeroelastic instabilities. However, the shrouds have an adverse effect on aerodynamic performance.

While the typical section model served the intended purposes, it is expected to be inadequate to obtain accurate flutter boundaries of modern technology turbofans or advanced turboprop blades which have a considerable amount of pretwist. As a consequence of pretwist, bending out of the plane of rotation couples elastically with bending in the plane of rotation. Consequently, a more realistic structural model of a blade is required.

The purposes of the research summarized herein, which is based in part on Ref. 4, are: 1) to develop a more refined and realistic structural model of a blade than the typical section model and to combine this model with the available unsteady cascade aerodynamic models, and 2) to study the effects of mistuning and other cascade parameters on flutter characteristics of an advanced technology fan stage. To the best of authors' knowledge, the mentioned effects utilizing the proposed model have not been studied in the published literature.

The structural dynamic model of the fan blade is complicated by the rotation of the blade. The rotation requires consideration of centrifugal softening and stiffening forces. The terms describing these forces in the equation of motion can be recovered only by either an explicit or implicit consideration of the geometric nonlinear theory of elasticity in deriving both the linear (first-degree terms in dependent variables) and the nonlinear (first- and higher-degree terms) equations of motion. Furthermore, if the blades are highly flexible (for example, helicopter blades) involving large deformations, some of the aeroelastic instabilities are associated with the second-degree structural and dynamic terms in the equations. In order to derive a consistent set of second-degree nonlinear aeroelastic equations, one also has to retain the second-degree terms in the unsteady cascade aerodynamic forces. Since an unsteady cascade aerodynamic theory including second-degree terms is not available, only linear terms in structural dynamic forces will be considered in this paper. Then, the structural dynamic model is essentially the same as that presented in Ref. 5.

The first-degree structural dynamic equations of a rotating pretwisted blade were developed in Ref. 5 by a Newtonian approach and by implicitly considering the geometric nonlinear theory of elasticity. Since that development, there have been misunderstandings and confusion about some of the terms in the equations of Ref. 5. To remove such misunderstandings and confusion, to account for disk radius, and for completeness, a brief summary of the development of a set of aeroelastic equations for a blade is presented. The development is characterized by the use of an extended Hamilton's principle in conjunction with an axial displacement which includes foreshortening[4] of the tension axis.

The disk is assumed to be rigid. The unsteady, two-dimensional, cascade, aerodynamic loads are calculated using Smith's theory[6] in subsonic flow and Adamczyk and Goldstein's theory[7] in supersonic flow with a subsonic leading edge. The governing equations of motion of a mistuned cascade are formulated by assuming that the general motion of a blade is a linear combination of its motions in all possible modes of a tuned cascade. The space variable in the coupled integro partial differential equations of motion is eliminated by using a modified Galerkin's method. The resulting equations are cast as a standard complex eigenvalue problem from which the aeroelastic stability is determined.

A digital computer program is developed to form and solve the complex eigenvalue problem. This program is written in a modular form such that it can be applied to advanced turboprops, helicopter rotors in hover, and wind turbine rotors by incorporating the appropriate aerodynamic modules. Due to length constraints of the paper, limited results are presented only for an advanced turbofan blade; however, additional parametric results will be presented in a future publication.

Theory

The components of a bladed disk system have complex geometries. The analysis of this system is complicated further by blade mistuning. To investigate the aeroelastic stability of

a cascade with mistuning, a mathematical model will be developed in this section.

Coordinate Systems

Several coordinate systems will be employed in the derivation of equations of motion; those which are common to both the structural and aerodynamic aspects of the derivation for the sth blade are shown in Figs. 1 and 2. The axis system $X_\Omega Y_\Omega Z_\Omega$ shown in the figures rotates with a constant angular velocity Ω about the X_Ω axis. The Y_Ω axis coincides with the undeformed elastic axis of the blade. The blade principal axes, x and z, of the cross section at an arbitrary point on the elastic axis are inclined to the X_Ω and Z_Ω axes by an angle ξ, as shown in Fig. 2. The blade elastic deformations u, v, w, and α translate and rotate the xyz system to the $x_3y_3z_3$ system, as shown in Fig. 1.

Tuned Cascade Model

If the blades are tuned, the N-bladed cascade has N interblade phase angle modes with a constant phase angle β_r between adjacent blades. This interblade phase angle is restricted by Lane's[8] assumption to the N discrete values $\beta_r = 2\pi r/N$ where $r = 0,1,2,\ldots,N-1$. In each of these modes all blades have the same amplitude. For a tuned cascade, the modes with different interblade phase angles are uncoupled. The blade deflections are expressed in a traveling-wave form in terms of a set of generalized coordinates which are associated with the nonrotating uncoupled beam modes in pure bending and torsion. The number of modes retained in the plane of rotation, in the plane perpendicular to the plane of rotation, and in torsion are M_h, M_q, and M_α, respectively. The blade deflections expressed in traveling-wave form are

$$\begin{Bmatrix} w/b_R \\ u/b_R \\ \alpha \end{Bmatrix} = [\bar{W}]\{X_s\}\exp[i(\omega/\omega_0)\tau]$$

$$= [\bar{E}_{s,r}][\bar{W}]\{Y_r\}\exp[i(\omega/\omega_0)\tau] \tag{1}$$

where

$$[\bar{W}] = \begin{bmatrix} W_1 & W_2 & \ldots & 0 & 0 & \\ 0 & 0 & \ldots & W_1 & W_2 & \ldots \\ 0 & 0 & \ldots & 0 & 0 & \ldots A_1, A_2 \ldots \end{bmatrix}$$

$$\{X_s\} = \{\bar{h}_{s1}\ \bar{h}_{s2}\ldots\bar{g}_{s1}\ \bar{g}_{s2}\ldots\alpha_{s1}\ \alpha_{s2}\ldots\}^T$$

$$\{Y_r\} = \{\bar{h}_{ar1}\ \bar{h}_{ar2}\ldots\bar{g}_{ar1}\ \bar{g}_{ar2}\ldots\alpha_{ar1}\ \alpha_{ar2}\ldots\}^T$$

$$[\bar{E}_{s,r}] = e^{i\beta_r s}[I] \tag{2}$$

An interblade phase angle β_r in the 0-180-deg range represents a forward-traveling wave, a wave traveling in the direction of rotation.

In Eq. (2) the standard nonrotating orthonormal modes for a beam with fixed-free boundary conditions are given by

$$W_j(\bar{\eta}) = \cosh(p_j\bar{\eta}) - \cos(p_j\bar{\eta})$$

$$- \frac{(\cos p_j + \cosh p_j)}{(\sin p_j + \sinh p_j)}[\sinh(p_j\bar{\eta}) - \sin(p_j\bar{\eta})] \tag{3}$$

$$A_j(\bar{\eta}) = \sqrt{2}\sin[(2j-1)\pi/2\bar{\eta}]$$

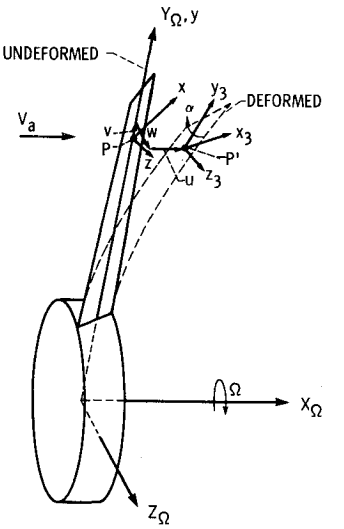

Fig. 1 Blade coordinate systems before and after deformation.

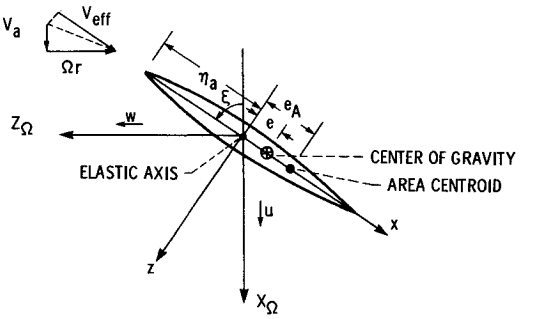

Fig. 2 Coordinate systems of blade cross section.

where the value of p_j is obtained from

$$\cos p_j \cosh p_j + 1 = 0 \tag{4}$$

In the case of a tuned cascade, it is adequate to analyze the motion of a cascade in each of the interblade phase angle modes separately. Hence, the total number of degrees of freedom of a tuned cascade is $(M_h + M_g + M_\alpha)$ for each value of β_r.

Mistuned Cascade Model

In the case of an arbitrarily mistuned cascade, the blades can have different amplitudes and the phase angle between adjacent blades can vary. However, the general motion of a blade in a mistuned cascade can be expressed as a linear combination of the motions in all possible interblade phase angle modes of the corresponding tuned cascade. Consequently, the blade deflections can be written as

$$\begin{Bmatrix} w/b_R \\ u/b_R \\ \alpha \end{Bmatrix} = [\bar{W}]\{X_s\}\exp[i(\omega/\omega_0)\tau]$$

$$= \sum_{r=0}^{N-1} [\bar{E}_{s,r}][\bar{W}]\{Y_r\}\exp[i(\omega/\omega_0)\tau] \tag{5}$$

For a case with N mistuned blades, Eq. (5) can be generalized as

$$[W]\{X\}\exp[i(\omega/\omega_0)\tau] = [E][W]\{Y\}\exp[i(\omega/\omega_0)\tau] \tag{6}$$

where

$$[W]=\begin{bmatrix}[\bar{W}] & & & \\ & [\bar{W}] & & \\ & & \ddots & \\ & & & [\bar{W}]\end{bmatrix}$$

$$\{X\}=\begin{Bmatrix}\{X_0\}\\ \{X_1\}\\ \vdots \\ \{X_{N-1}\}\end{Bmatrix} \qquad \{Y\}=\begin{Bmatrix}\{Y_0\}\\ \{Y_1\}\\ \vdots \\ \{Y_{N-1}\}\end{Bmatrix}$$

$$[E]=\begin{bmatrix}[\bar{E}_{0,0}] & [\bar{E}_{0,1}] & \cdots \\ [\bar{E}_{1,0}] & [\bar{E}_{1,1}] & \cdots \\ \vdots & \vdots & [\bar{E}_{n-1,N-1}]\end{bmatrix} \tag{7}$$

The total number of degrees of freedom for this general case is N times $(M_h+M_g+M_\alpha)$.

Aerodynamic Model

The unsteady, two-dimensional, cascade, aerodynamic loads were calculated by using Smith's theory in subsonic flow, and Adamczyk and Goldstein's[7] theory in supersonic flow with a subsonic leading edge. In these theories, the airfoil thickness, camber, and steady-state angle of attack are neglected, and the flow is assumed to be isentropic and irrotational. At any radial station the relative Mach number is a function of the inflow conditions and rotor speed. Most current fan designs have supersonic flow at the tip and subsonic flow at the root. As a result, some region of the blade span encounters transonic flow. Since the above unsteady theories are not valid in the transonic region, the subsonic theory with $M_{\text{eff}}=0.9$ for stations in the range $0.9\le M_{\text{eff}}<1$ and the supersonic theory with $M_{\text{eff}}=1.1$ for stations in the range $1.0\le M_{\text{eff}}\le 1.1$ were used. The motion-dependent aerodynamic lift and moment were expressed in Ref. 1 in terms of nondimensional coefficients, l_{hhr}, $l_{h\alpha r}$, $l_{\alpha hr}$, and $l_{\alpha\alpha r}$. The expressions for lift and moment per unit span as a function of the same coefficients and the mode shapes described in Eqs. (3) and (4) can be derived following the procedure used in Ref. 9 and are

$$L_a=-\pi\rho_a b_R^3\omega^2\sum_{r=0}^{N-1}\left\{l_{hhr}\left(\frac{b}{b_R}\right)^2\left[\cos\xi\sum_{j=1}^{M_h}W_j(\bar{\eta})\bar{h}_{arj}+\sin\xi\sum_{j=1}^{M_g}W_j(\bar{\eta})\bar{g}_{arj}\right]+l_{h\alpha r}\left(\frac{b}{b_R}\right)^3\sum_{j=1}^{M_\alpha}A_j(\bar{\eta})\alpha_{arj}\right\}\times\exp\left[i\left(\frac{\omega}{\omega_0}\tau+\beta_r s\right)\right] \tag{8a}$$

$$M_a=\pi\rho_a b_R^4\omega^2\sum_{r=0}^{N-1}\left\{l_{\alpha hr}\left(\frac{b}{b_R}\right)^3\left[\cos\xi\sum_{j=1}^{M_h}W_j(\bar{\eta})\bar{h}_{arj}+\sin\xi\sum_{j=1}^{M_g}W_j(\bar{\eta})\bar{g}_{arj}\right]+l_{\alpha\alpha r}\left(\frac{b}{b_R}\right)^4\sum_{j=1}^{M_\alpha}A_j(\bar{\eta})\alpha_{arj}\right\}\times\exp\left[i\left(\frac{\omega}{\omega_0}\tau+\beta_r s\right)\right] \tag{8b}$$

The coefficients $l_{hhr}, l_{h\alpha r},\ldots,l_{\alpha\alpha r}$ are calculated for specified values of M_{eff}, k, s/c, ξ, and a. In the aerodynamic theories used herein, the steady-state angle of attack is neglected. In applying these theories to the present case, the blade steady-state angle of attack is also set to zero and the effective relative velocity is assumed to be the component of the blade relative velocity along the blade chord, as indicated in Fig. 2.

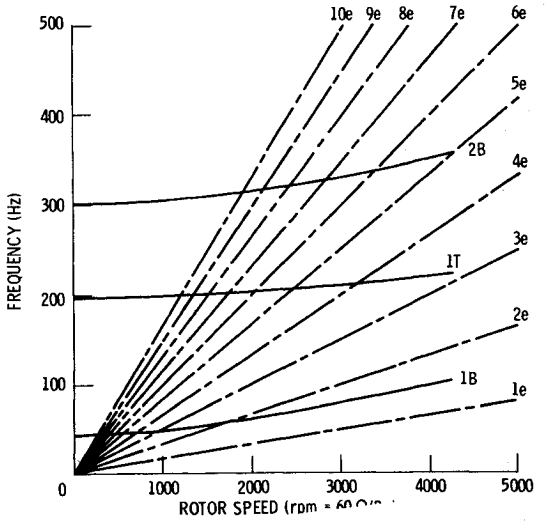

Fig. 3 Campbell diagram of the fan blade.

Structural Model

The structural model of each blade consists of a straight, slender, twisted, nonuniform elastic beam with a symmetric cross section. The elastic, inertia, and tension axes are taken to be noncoincident. The effect of warping is not explicitly considered. However, a partial effect of warping enters into the equations of motion, as shown in Ref. 5. The blade is assumed to be rigid in the direction along the elastic axis. Consequently, the axial equation of motion is eliminated. The

Table 1 Blade sectional properties

	$\bar{\eta}$							
	0.0199	0.1017	0.2372	0.4083	0.5917	0.7628	0.8983	0.9801
$\bar{EI}_{xx}$	0.9719	0.9665	0.7827	0.6072	0.3067	0.1633	0.1149	0.0839
$\bar{EI}_{zz}$	112.4	124.8	152.4	139.4	122.7	119.3	127.7	124.1
$\bar{GJ}$	0.9719	0.9665	0.7827	0.6072	0.3067	0.1633	0.1149	0.0839
$\bar{EA}$	0.9974	1.0225	0.9711	0.9358	0.7641	0.6482	0.6038	0.5541
$\bar{EB}_1$	0.4436	0.5338	0.5675	0.7275	0.6901	0.7694	0.9458	0.9734
$\bar{EB}_2$	0.0	0.0	0.0	0.0	0.0	0.0	0.0	0.0
$\bar{e}$	0.0	0.0	0.0	0.0	0.0	0.0	0.0	0.0
$\bar{e}_A$	0.0	0.0	0.0	0.0	0.0	0.0	0.0	0.0
$\bar{k}_A$	0.5859	0.6095	0.6265	0.6722	0.6972	0.7461	0.7995	0.8226
$\bar{k}_{m_1}$	0.0940	0.0925	0.0854	0.0767	0.0603	0.0478	0.0415	0.0370
$\bar{k}_{m_2}$	1.0103	1.0516	1.0816	1.1616	1.2060	1.2913	1.3840	1.4242
$\bar{m}$	0.9974	1.0225	0.9711	0.9358	0.7641	0.6482	0.6038	0.5541
$\bar{b}$	1.010	1.051	1.082	1.161	1.206	1.291	1.384	1.425

structural model has its basis in the geometric nonlinear theory of elasticity in which elongations and shears are negligible compared to unity and the squares of the derivatives of the extensional deformation of the elastic axis are negligible compared to the squares of the bending slopes. This level of the geometric nonlinear theory of elasticity is required to derive a set of linear coupled bending-torsion equations of motion.

Equations of Motion

The equations of motion will be derived by using the extended Hamilton's principle in the form

$$\int_{t_0}^{t_1} (\delta T_k - \delta U + \delta W)\,\mathrm{d}t = 0 \tag{9}$$

The expression for strain energy, kinetic energy, and virtual work of aerodynamic forces can be written as

$$U = \frac{1}{2}\int_{R_H}^{R_T}\iint_A [E\gamma_{yy}^2 + G(\gamma_{yz}^2 + \gamma_{yx}^2)]\,\mathrm{d}r\mathrm{d}x\mathrm{d}z \tag{10}$$

$$T_k = \frac{1}{2}\int_{R_H}^{R_T}\iint_A \rho_m \frac{\mathrm{d}\bar{r}_1}{\mathrm{d}t}\cdot\frac{\mathrm{d}\bar{r}_1}{\mathrm{d}t}\,\mathrm{d}r\mathrm{d}x\mathrm{d}z \tag{11}$$

$$\delta W = \int_{R_H}^{R_T} (-L_a\sin\xi\,\delta u - L_a\cos\xi\,\delta w + M_a\delta\alpha)\,\mathrm{d}r \tag{12}$$

where

$$\frac{\mathrm{d}\bar{r}_1}{\mathrm{d}t} = \frac{\partial\bar{r}_1}{\partial t} + \bar{\omega}\times\bar{r}_1$$

$$\bar{\omega} = \Omega(\bar{e}_x\cos\xi + \bar{e}_z\sin\xi)$$

$$\bar{r}_1 = (r - U_F)\bar{e}_y + (u\cos\xi - w\sin\xi)\bar{e}_x$$

$$+ (u\sin\xi + w\cos\xi)\bar{e}_z + \begin{Bmatrix}\bar{e}_x\\ \bar{e}_y\\ \bar{e}_z\end{Bmatrix}^T [T]^T \begin{Bmatrix}x\\ r\\ z\end{Bmatrix} \tag{13}$$

The expressions for the strain components, position vector, foreshortening, and transformation matrix are developed in Ref. 4. Substituting those expressions into Eq. (10), Eq. (13) into Eq. (11), Eqs. (8a) and (8b) into Eq. (12), the resulting equations into Eq. (9), taking the indicated variations, integrating over the cross section of the blade wherever necessary, integrating by parts over time, neglecting Coriolis and rotary inertia terms, and retaining only first-degree terms in u, w, and α yields

$$[(EI_{zz}\sin^2\xi + EI_{xx}\cos^2\xi)w'' - (EI_{zz} - EI_{xx})u''\sin\xi\cos\xi$$
$$- EB_2\xi'\alpha'\sin\xi - T_c e_A\alpha\cos\xi]'' - (T_c w')' + m\ddot{w} + me\ddot{\alpha}\cos\xi$$
$$- \Omega^2[(mre\alpha\cos\xi)' + mw + me\alpha\cos\xi] = -L_a\cos\xi \tag{14a}$$

$$[(EI_{zz}\cos^2\xi + EI_{xx}\sin^2\xi)u'' - (EI_{zz} - EI_{xx})w''\sin\xi\cos\xi$$
$$+ EB_2\xi'\alpha'\cos\xi - T_c e_A\alpha\sin\xi]'' - (T_c u')'$$
$$+ m\ddot{u} + me\ddot{\alpha}\sin\xi - \Omega^2(mre\alpha\sin\xi)' = -L_a\sin\xi \tag{14b}$$

$$-[GJ\alpha' + EB_1\xi'^2\alpha' + T_c k_A^2\alpha' + EB_2\xi'(u''\cos\xi$$
$$- w''\sin\xi)]' - T_c e_A w''\cos\xi - T_c e_A u''\sin\xi$$
$$+ m(k_m^2\ddot{\alpha} + e\ddot{u}\sin\xi + e\ddot{w}\cos\xi) + m\Omega^2 re(w'\cos\xi$$
$$+ u'\sin\xi) - m\Omega^2[(k_{m_2}^2 - k_{m_1}^2)\alpha\cos 2\xi + we\cos\xi] = M_a \tag{14c}$$

The sectional properties in these equations are defined in Appendix A.

By substituting Eqs. (8a) and (8b) into Eqs. (14), nondimensionalizing the resulting equations, applying Galerkin's method, and extending the resultant equations to all of the blades by using Eq. (6), the equations of motion of an arbitrarily mistuned cascade can be simplified as

$$[P]\{Y\} = \gamma[Q]\{Y\} \tag{15}$$

where

$$[Q] = [E]^{-1}[M][E] + [A]$$

$$[P] = [E]^{-1}[S][E]$$

$$\gamma = (\omega/\omega_0)^2 \tag{16}$$

The expressions for the mass matrix $[M]$, stiffness matrix $[S]$, for aerodynamic matrix $[A]$ are given in Ref. 4. It should be mentioned that in the stiffness matrix, the structural damping is added by multiplying the direct stiffness coefficients by $(1+2i\zeta_{hs1})$, $(1+2i\zeta_{hs2})$,...,$(1+2i\zeta_{\alpha s1})$, etc. The sectional and nondimensional variable properties used in Eqs. (15) and (16) are listed in Appendices A and B, respectively.

Solution

The aeroelastic stability boundaries are obtained by solving the standard complex eigenvalue problem represented by Eq. (15). The relation between the frequency ω and γ is

$$i(\omega/\omega_0) = i\sqrt{\gamma} = \bar{\mu} \pm i\bar{\nu} \tag{17}$$

Flutter occurs when $\bar{\mu} > 0$.

Computer Program and Verification

A computer program (ASTROMIC) was written to assemble and solve the generalized eigenvalue problem given in Eq. (15). The program can be used to predict the in-vacuum natural frequencies of a nonuniform rotating beam by setting the aerodynamic matrix $[A]$ to zero. In this case the problem is reduced to a standard eigensolution. For the flutter problem, the aerodynamic matrix is a function of the eigenvalues. Hence, an iterative solution is required. The iterative technique used herein to calculate flutter boundaries (once the problem is completely described) is briefly summarized as follows:

1) Select an axial Mach number.

2) Select a rotation speed and assemble the stiffness and mass matrices.

3) Calculate the variation of the reduced frequency based on an assumed reference frequency ω_0 and relative Mach number with span and construct the aerodynamic matrix. The initial value for the reference frequency is the same as the natural frequency of the mode of interest.

4) Solve the eigenvalue problem.

5) For the mode of interest check whether the imaginary part of the eigenvalue is within an acceptable tolerance of the reference frequency. If not, go back to step 3 with a new reference frequency.

6) For the mode of interest, check whether the real part of the eigenvalue is within an acceptable tolerance of zero. If not, modify the rotational speed and repeat the process from step 2. If positive, reduce speed; if negative, increase speed.

7) To find the flutter boundary for another value of the axial Mach number go back to step 1.

It should be noted that the above method utilizes a rotor speed iteration within the axial Mach number iteration loop. It would appear that it would be more efficient to place the Mach number iteration within the rotor speed iteration loop since the mass and stiffness matrices have to be updated each time the rotor speed is changed. However, it was found that the time required to assemble these matrices is small relative to the time required to assemble the aerodynamic matrix and to extract the eigenvalues and eigenvectors. In addition, the flutter boundary was more "distinct" using the method described above.

The correctness of the program was checked by constructing a hypothetical blade model with constant structural and aerodynamic properties along the span. The blade frequencies obtained using the program were checked against known solutions. The eigensolutions with aerodynamics included were checked against the results obtained using the typical section model program (MISER) developed in Refs. 1 and 2.

For a cascade with nonuniform blades there are no published theoretical results on flutter. However, the results from ASTROMIC are compared with those from MISER by choosing the properties for a typical section at different spanwise stations. These results will be discussed later.

Aeroelastic Stability of an Advanced Fan

An advanced unshrouded fan stage (aspect ratio = 3.3) representative of a next-generation fan was chosen for analysis. A similar stage was analyzed in Ref. 3 using the typical section model. The results in Ref. 3 indicated that the fan design without shrouds did not meet the flutter requirements, but that it may be feasible to use mistuning as a passive flutter control. The motivation for choosing this fan stage for analysis herein is to further investigate the use of mistuning as a passive flutter control.

The properties of the fan blade are listed in Table 1, and the reference properties are listed in Table 2. The design point is at a rotor speed of 4267 rpm and an axial Mach number of 0.55. At these conditions the tip relative Mach number is 1.45.

The analyses are performed using two modes each in the plane of rotation, in the plane perpendicular to the plane of rotation, and in torsion. Since there are 28 blades in this stage and, hence, 28 interblade phase angle modes, the total number of degrees of freedom for an arbitrarily mistuned cascade is 168. However, for alternate mistuning, in which every other blade is identical, certain symmetry properties are exploited in the analysis. Because of symmetry, the β_r mode couples with the $(\beta_r + \pi)$ mode only. The analysis for this case consists of 14 separate eigensolutions of 12 degrees of freedom each rather than one eigensolution of 168 degrees of freedom for an arbitrarily mistuned cascade.

The blade was analyzed for vibration to generate a Campbell diagram shown in Fig. 3. Only the first and second bending frequencies and the first torsion frequency are shown. Since the mass ratio for this blade is high, the aerodynamic forces result in flutter frequencies which are not significantly different from those in a vacuum.

In Refs. 1-3, a typical section model, which was used originally for fixed-wing flutter analysis, was adapted for rotating blades. In the case of a fixed wing, the relative velocity of each strip along the span is constant; the structural properties of the typical section are obtained by their respective values at the three-quarter blade span station. In the case of a rotating blade, the relative velocity of each strip along the blade varies. Then, a question arises as to which spanwise station should be used as a reference to calculate the structural and aerodynamic properties of the typical section. To answer this question, the eigenvalues of the tuned cascade at the design condition from both the present beam and typical section analyses using various spanwise locations as reference are compared in Fig. 4. As expected, the cascade is unstable over a range of interblade phase angles corresponding to forward-traveling waves. It should be noted that, whereas there are 168 eigenvalues, only the predominantly torsional eigenvalues are shown. The other modes were found to be stable at the design condition. Also, it

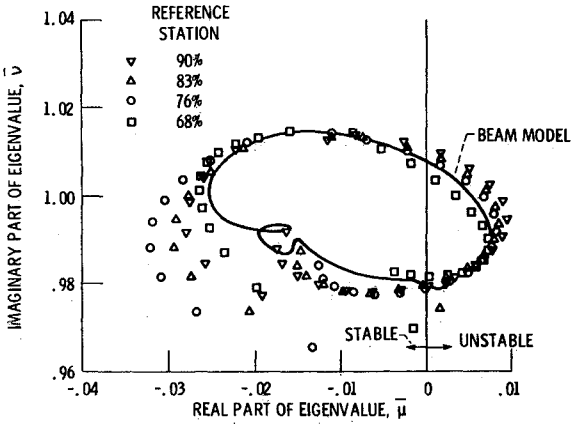

Fig. 4 Comparison of eigenvalues from beam model and typical section models: $\omega_0 = 1409.6$ rad/s, $\Omega = 446.8$ rad/s, $M_{ax} = 0.55$.

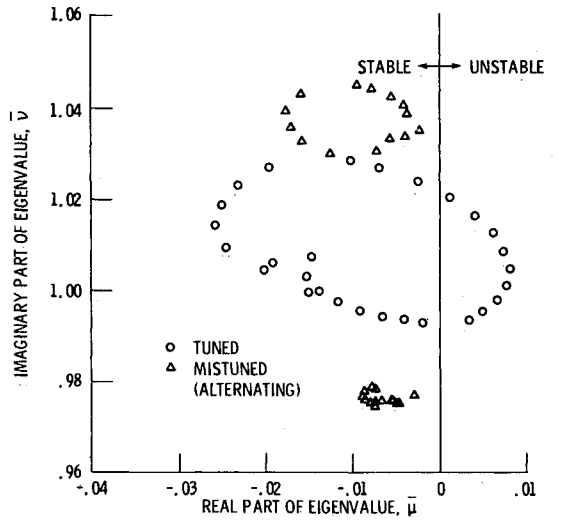

Fig. 5 Comparison of eigenvalues of tuned and mistuned cascade: $\omega_0 = 1391.1$ rad/s, $\Omega = 446.8$ rad/s, $M_{ax} = 0.55$.

Table 2 Reference quantities

$N = 28$	$\rho_m = 4374$ kg/m^3
$b_R = 0.0946$ m	$\rho_a = 1$ kg/m^3
$R_H = 0.3876$ m	$a_0 = 340.3$ m/s
$R_T = 1.021$ m	$A_0 = 0.0034$ m^2
$E = 1.23 \times 10^{11}$ N/m^2	$r_{\alpha 0} = 0.5774$
$G = 4.744 \times 10^{10}$ N/m^2	$\omega_0 =$ varies, rad/s
$I_{xx0} = 9.19 \times 10^{-8}$ m^4	$M_h = M_g = M_\alpha = 2$
$J_0 = 3.676 \times 10^{-7}$ m^4	$\xi = \tan^{-1}[1.552\,(\bar{\eta} + \bar{e}_H)]$

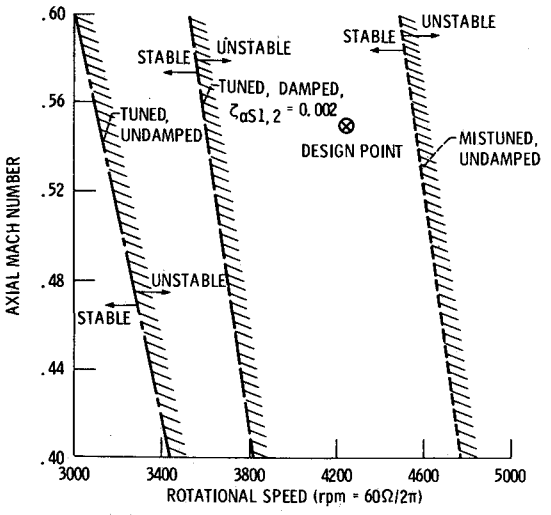

Fig. 6 Comparison of tuned and mistuned flutter boundaries.

can be seen that the typical section model corresponding to approximately the 7/10 span reference station gives the best correlation for the unstable modes with the nonuniform blade model. This finding is in close agreement with the three-quarter span reference station usually used for fixed-wing aeroelastic calculations. This observation is very useful in performing preliminary aeroelastic analyses.

Previous publications[1-3] using the typical section model have shown that torsional frequency mistuning could have a significant stabilizing effect on the cascade. The effect of mistuning is further investigated herein with the nonuniform blade model. The method used to vary the frequency from blade to blade was simply to vary the torsional stiffness, J. For alternate mistuning, the torsional stiffness of the odd numbered blades was increased by 10% over that of a tuned blade at each spanwise location. Likewise, the torsional stiffness of the even numbered blades was decreased by 10% from that of a tuned blade. The result was a total torsional frequency variation of approximately 7%. The eigenvalues for this mistuned rotor at the design conditions are shown in Fig. 5, along with the corresponding tuned values. These predominately torsional eigenvalues have split into high- and low-frequency families corresponding to modes with major participation of the odd and even blades, respectively. As can be seen, this type of mistuning has stabilized the cascade to such an extent that it is stable at the design point.

By using the iterative procedure defined above, the flutter boundaries for both the tuned and mistuned cascades were calculated. The results are shown in Fig. 6. For the tuned cascade it is seen that the design point lies well inside in the unstable region. As expected, the axial Mach number at flutter monotonically decreases with increasing rotor speed. For the tuned cascade it should also be noted that along the flutter boundary the tip relative Mach number is approximately 1.15. Consequently, a region near the blade tip may experience nonlinearities associated with transonic flow which are not accounted for by the unsteady aerodynamic theories used herein. The relative tip Mach number at the design conditions is 1.45.

The inclusion of an alternate frequency mistuning of approximately 7% has increased the cascade stability significantly by moving the flutter boundary to the right. Furthermore, the design point is stable for this level of mistuning. The mode defining the boundary has maximum participation of the even numbered (or low-frequency) blades. The tip relative Mach number along the boundary of the mistuned cascade is 1.53. Consequently, the transonic region is considerably inboard of the tip and the transonic effects should be minimal.

Figure 6 also illustrates the effect of structural damping on flutter of a tuned cascade. A structural damping ratio of 0.002 is included in each of the torsional modes. As can be seen, the damping has a significantly stabilizing effect on flutter speed of a tuned cascade.

Conclusions

The major conclusions from this investigation are summarized as follows:

1) An aeroelastic model and an associated computer program for a mistuned cascade with nonuniform blades were developed.

2) For the blade analyzed herein, a typical section model corresponding to the 7/10 span reference station gives the best correlation with the nonuniform blade model.

3) An advanced, unshrouded, high-aspect-ratio fan was modeled and analyzed with and without mistuning. The results show that a moderate amount of mistuning has enough potential to alleviate flutter problems in unshrouded turbofans.

Appendix A: Sectional Properties and Definition of Matrices

$$T_c = \int_r^{R_T} m\Omega^2 r\,dr, \qquad I_{xx} = \iint z^2\,dx\,dz$$

$$I_{zz} = \iint x^2\,dx\,dz - e_A^2 A, \qquad B_1 = \iint (x^2 + z^2 - k_A^2)^2\,dx\,dz$$

$$B_2 = \iint (x - e_A)(x^2 + z^2 - k_A^2)\,dx\,dz, \qquad J = \frac{ct^3}{3}$$

$$A = \iint dx\,dz, \qquad Ae_A = \iint x\,dx\,dz$$

$$Ak_A^2 = \iint (x^2 + z^2)\,dx\,dz, \qquad m = \iint \rho_m\,dx\,dz$$

$$me = \iint \rho_m x\,dx\,dz, \qquad mk_{m_1}^2 = \iint \rho_m z^2\,dx\,dz$$

$$mk_{m_2}^2 = \iint \rho_m x^2\,dx\,dz, \qquad k_m^2 = k_{m_1}^2 + k_{m_2}^2$$

Appendix B: Nondimensional Quantities

$$\bar{\eta} = \frac{r - R_H}{L} = \frac{\eta}{L} \qquad \bar{e}_A = e_A/b_R$$

$$\bar{b} = b/b_R \qquad \bar{e} = e/b_R$$

$$\bar{h}_s = h_s/b_R \qquad \bar{e}_H = R_H/L$$

$$\bar{g}_s = g_s/b_R \qquad \overline{T_c} = T_c/m_0\Omega^2 L^2$$

$$\tau = t\omega_0 \qquad \overline{EB_1} = EB_1/GJ_0L^2$$

$$\overline{EI_{xx}} = EI_{xx}/EI_{xx0} \qquad \overline{EB_2} = EB_2/GJ_0L$$

$$\overline{EI_{zz}} = EI_{zz}/EI_{xx0} \qquad \bar{k}_m = k_m/k_{m_0}$$

$$\overline{GJ} = GJ/GJ_0 \qquad \bar{k}_{m_1} = k_{m_1}/k_{m_0}$$

$$\overline{EA} = EA/EA_0 \qquad \bar{k}_{m_2} = k_{m_2}/k_{m_0}$$

$$\bar{m} = m/m_0$$

References

[1]Kaza, K. R. V. and Kielb, R. E., "Effects of Mistuning on Bending-Torsion Flutter and Response of a Cascade in Incompressible Flow," AIAA Paper 81-0532; also, *AIAA Journal*, Vol. 20, Aug. 1982, pp. 1120-1127.

[2]Kielb, R. E. and Kaza, K. R. V., "Aeroelastic Characteristics of a Cascade of Mistuned Blades in Subsonic and Supersonic Flows," ASME Paper 81-DET-122, Sept. 1981; also, *ASME Journal of Vibration, Acoustics, Stress and Reliability of Design*, Vol. 105, Oct. 1983, pp. 425-433.

[3]Kielb, R. E., "Aeroelastic Characteristics of a Mistuned Bladed-Disc Assembly," Ph.D. Dissertation, The Ohio State University, Columbus, Ohio, 1981.

[4]Kaza, K. R. V. and Kielb, R. E., "Coupled Bending-Bending-Torsion Flutter of Mistuned Cascade with Nonuniform Blades," AIAA Paper 82-0726, *Proceedings of the AIAA/ASME/ASCE/AHS 23rd Structures, Structural Dynamics and Materials Conference*, New Orleans, La., May 1982, pp. 446-461.

[5]Houbolt, J. C. and Brooks, G. W., "Differential Equations of Motion for Combined Flapwise Bending, Chordwise Bending, and Torsion of Twisted Nonuniform Rotor Blades," NACA Rept. 1346, 1958.

[6]Smith, S. N., "Discrete Frequency Sound Generation in Axial Flow Turbomachines," ARC R&M 3709, 1973.

[7]Adamczyk, J. J. and Goldstein, M. E., "Unsteady Flow in Supersonic Cascade with Subsonic Leading-Edge Locus," *AIAA Journal*, Vol. 16, Dec. 1978, pp. 1248-1254.

[8]Lane, F., "System Mode Shapes in the Flutter of Compressor Blade Rows," *Journal of the Aeronautical Sciences*, Vol. 23, Jan. 1956, pp. 54-56.

[9]Scanlan, R. H. and Rosenbaum, R., *Aircraft Vibration and Flutter*, Dover Publications, Inc., N.Y., 1968.

From the AIAA Progress in Astronautics and Aeronautics Series..

RAREFIED GAS DYNAMICS: PART I AND PART II—v. 51

Edited by J. Leith Potter

Research on phenomena in rarefied gases supports many diverse fields of science and technology, with new applications continually emerging in hitherto unexpected areas. Classically, theories of rarefied gas behavior were an outgrowth of research on the physics of gases and gas kinetic theory and found their earliest applications in such fields as high vacuum technology, chemical kinetics of gases, and the astrophysics of interstellar media.

More recently, aerodynamicists concerned with forces on high-altitude aircraft, and on spacecraft flying in the fringes of the atmosphere, became deeply involved in the application of fundamental kinetic theory to aerodynamics as an engineering discipline. Then, as this particular branch of rarefied gas dynamics reached its maturity, new fields again opened up. Gaseous lasers, involving the dynamic interaction of gases and intense beams of radiation, can be treated with great advantage by the methods developed in rarefied gas dynamics. Isotope separation may be carried out economically in the future with high yields by the methods employed experimentally in the study of molecular beams.

These books offer important papers in a wide variety of fields of rarefied gas dynamics, each providing insight into a significant phase of research.

Volume 51 sold only as a two-volume set
Part I, 658 pp., 6x9, illus.
Part II, 679 pp., 6x9, illus.
$37.50 Member, $70.00 List

TO ORDER WRITE: Publications Dept., AIAA, 1633 Broadway, New York, N.Y. 10019